Available online at www.sciencedirect.com
SCIENCE DIRECT®
Journal of Sound and Vibration 287 (2005) 405–431
JOURNAL OF SOUND AND VIBRATION
www.elsevier.com/locate/jsvi

Modal analysis of the human neck in vivo as a criterion for crash test dummy evaluation

R. Willinger[a,*], N. Bourdet[a], R. Fischer[a], F. Le Gall[b]

[a]*UMR 7507 ULP-CNRS, University of Strasbourg, 2 rue Boussingault, 67000 Strasbourg, France*
[b]*CERA-TREVES, rue Emile Arquès, 51000 Reims, France*

Received 21 May 2003; received in revised form 25 October 2004; accepted 4 November 2004
Available online 19 January 2005

Abstract

Low speed rear impact remains an acute automative safety problem because of a lack of knowledge of the mechanical behaviour of the human neck early after impact. Poorly validated mathematical models of the human neck or crash test dummy necks make it difficult to optimize automotive seats and head rests. In this study we have constructed an experimental and theoretical modal analysis of the human head–neck system in the sagittal plane. The method has allowed us to identify the mechanical properties of the neck and to validate a mathematical model in the frequency domain. The extracted modal characteristics consist of a first natural frequency at 1.3 ± 0.1 Hz associated with head flexion-extension motion and a second mode at 8 ± 0.7 Hz associated with antero-posterior translation of the head, also called retraction motion. Based on this new validation parameters we have been able to compare the human and crash test dummy frequency response functions and to evaluate their biofidelity. Three head–neck systems of current test dummies dedicated for use in rear-end car crash accident investigations have been evaluated in the frequency domain. We did not consider any to be acceptable, either because of excessive rigidity of their flexion-extension mode or because they poorly reproduce the head translation mode. In addition to dummy evaluation, this study provides new insight into injury mechanisms when a given natural frequency can be linked to a specific neck deformation.

*Corresponding author. Tel.: +33 3 90 242923; fax: +33 3 88 61 43 00.
E-mail addresses: willi@imfs.u-strasbg.fr (R. Willinger), bourdet@imfs.u-strasbg.fr (N. Bourdet), fischer@imfs.u-strasbg.fr (R. Fischer), francois.legall@treves.fr (F. Le Gall).

0022-460X/$ - see front matter © 2004 Elsevier Ltd. All rights reserved.
doi:10.1016/j.jsv.2004.11.008

1. Introduction

Despite advances in safety devices, neck injuries in traffic accidents, especially non-severe rear impact accidents, continue to be a serious and costly social problem. The high cost of whiplash injury has been extensively documented in several countries [1,2]. The development of safety measures designed to decrease the incidence of whiplash injuries must be guided by meaningful and reliable human body surrogates. Most injury prevention strategies are based on impact analysis using anthropomorphic crash test dummies or mathematical models. Without proper evaluation of these experimental and computational models against the mechanical responses of the human body, it will not be possible to improve current state-of-the-art neck injury prevention techniques. Unfortunately the cervical spine is one of the most complex structures in the human skeletal system and its behaviour during impact is still poorly understood.

At present there are no less than three crash test dummies dedicated for use in experimental rear impact analysis. The Hybrid III dummy developed by [3], the BioRID II designed at Chalmers University [4] and the RID dummy proposed by TNO in the Netherlands [5]. A number of validation studies have been conducted on these dummies against volunteers and against post mortem subject neck responses [4–10] and have demonstrated the limited biofidelity of this human body surrogate under low speed rear impact. Optimization studies of the car-seat-head rest system are also described [1,11–13] and conclude that the safest protective system against whiplash depends on the dummy used.

Mathematical models of the head–neck system have also been described, although validation difficulties remain. Initially, lumped models were proposed with elastic-damped pivot joints and inertial data [14,15]. This type of model became more and more sophisticated, leading to rigid mathematical models [16,17]. In the last few decades, several finite element models (FE models) of the cervical column have been proposed in order to more accurately simulate the response of the neck under impact. However, as with analytical modelling, the utility of FE models depends on their biofidelity. Nowadays, although attractive models have been developed, modelling of neck kinematics remains imperfect [18–20] and needs improved representation of the dynamic response, particularly in rear impact conditions, for which only two models have even been partially validated [21,22].

Typically, numerical or physical neck model validation is conducted on volunteers or on post mortem human subjects (PMHS) by comparing the changes in several recorded mechanical parameters over time with the human response. This methodology is limited as it is very difficult to characterize a multiple degrees of freedom system under impact in the temporal domain. These difficulties are well illustrated by the large number of test dummy evaluation and comparative studies found in the literature. The number of prototype versions and contradictions between study conclusions described illustrate how difficult it is to explain some phenomena that are masked within the time domain. The reason for this is that the dummy response has to remain within ranges or corridors, which have wide tolerance. The evaluation process in the temporal domain is not sufficiently accurate to extract initial ramps, local peaks and oscillations that can be of great importance.

Despite this critical issue, recent research in head–neck biomechanics has improved our knowledge of this complex structure. The limitations listed above illustrate the need for further experimental and theoretical analysis. The purpose of this paper is to apply modal analysis

techniques to characterize the head–neck system in vivo and to derive new methods for model identification. The method is then subsequently applied to existing dummy evaluation.

Under rear end impact conditions, the human neck has been characterized experimentally by decelerating a human subject seated in a car, with or without a headrest [12,23]. The loading conditions or inputs in these experiments were defined by a sled speed (5–13 km/h) or more usefully by the first thoracic vertebra acceleration (2–5-g over 80–150 ms). The neck response is recorded in terms of head kinematics such as linear acceleration (3–8 g over 80–100 ms). More recently Ono et al. [24] suggested characterizing the human cervical spine by directly loading the head with a force close to 150 N (over 50 ms) applied horizontally to the front or vertically to the chin. Although Ono's investigation is focused on a study of the response of the head under air bag deployment, it does however examine dummy neck biofidelity evaluation in the sagittal plane.

This study seeks to characterize the head–neck system under similar inputs (150 N; 3 g; 50 ms) by loading the forehead directly and recording its kinematics. This loading condition produces a rearward motion of the head, which in turn allows the mechanical properties of the head–thorax junction to be examined in the sagittal plane. The novel feature of this study is that it ignores the temporal analysis and undertakes a frequency analysis of the head–neck response, followed by extraction of the system's modal characteristics inherent to the system regardless of loading. Accordingly, it is accepted that the modal behaviour of a system under study does not depend on the loading condition although its temporal response clearly does. Finally, modal analysis is a powerful tool for identification of parameters that enable validation of the model over a wide range of loading rates, whereas investigation in the time domain often produces nonlinear models validated for a limited number of impacts.

Modal analysis is currently used in engineering for non-destructive identification of dynamic structure. In biomechanics the method has been used extensively for bone healing processing and for dynamic characterization of the human head [25–27]. With respect to the spinal column, and in addition to impedance recording of a single degree of freedom, Kitazaki et al. [28] undertook a detailed theoretical and experimental modal analysis of the whole column including the head. A total of 15 degrees of freedom were taken into account, 3 for the head, 10 for the spinal column and 2 for the frontal area of the abdomen. The seated subject was vibrated vertically. The transfer function in terms of the apparent mass between the input force and the different degrees of freedom accelerations made it possible to extract the modal characteristics of the system in the modal domain, i.e. natural frequencies and Eigen vectors or mode shapes. In this way, eleven vibration modes were identified between 1.8 and 17 Hz due to back movements. The aim of this study was comfort study and modal characterization. The modelling was therefore restricted to definition of the analytical transfer function rather than mechanical characterization of the human body. Conversely, the choice of degrees of freedom was not tailored to neck investigation and no mode shapes, natural frequencies or mechanical properties of the neck were therefore investigated. The main objective of this study is to examine these latter parameters.

The experimental modal analysis of the human head–neck system in vivo obtained from this study will provide us with natural frequencies and mode shapes which must be reproduced by the dummy head–neck system. Initially we describe the technique applied to human volunteer subjects and demonstrate how this experiment provides the biomechanical background for the proposed dummy evaluation methodology. Experimental modal analysis is then applied to three existing rear impact test dummies under similar loading conditions as the volunteers. The discussion

endeavours to bring together the results obtained with issues arising from temporal investigations and to examine the implications of the study.

2. Experimental modal analysis of the head–neck system

In this section, modal characterization of the head–neck system in vivo is described for five healthy volunteers (25–48 years old) all without disease of the cervical spine. The testing protocol was approved under the relevant laws and regulations of our institution. All subjects underwent a medical check prior to the experiments and were questioned about any symptoms of any nature, which developed after the experiments. None of the subjects complained of any discomfort.

The experimental device shown in Fig. 1 consists of a pendulum articulated on a gantry which impacts frontally onto the volunteer's forehead with a basketball. The volunteer is seated on a rigid seat without a headrest. The subject's shoulders are firmly held against the backrest of the seat in order to avoid contributions from movement of the torso. In this experimental configuration, the volunteers were asked to close eyes and to relax the muscles of their neck during the entire test (RElaxed Condition), in order to avoid contribution from the muscles. It is assumed that head motion remains in the sagittal plane with a sufficiently small amplitude (a few degrees) that the applied frontal force and recorded linear acceleration can be assumed to be unidirectional in the antero-posterior direction. Head acceleration is measured using nine accelerometers (Entran EGA ± 10 g) arranged in the well-known 3-2-2-2 configuration as shown in Fig. 2, in order to calculate the linear component of head acceleration at any point. The impulse force is recorded using a force sensor (PCB 208A02 11.432 mV/N).

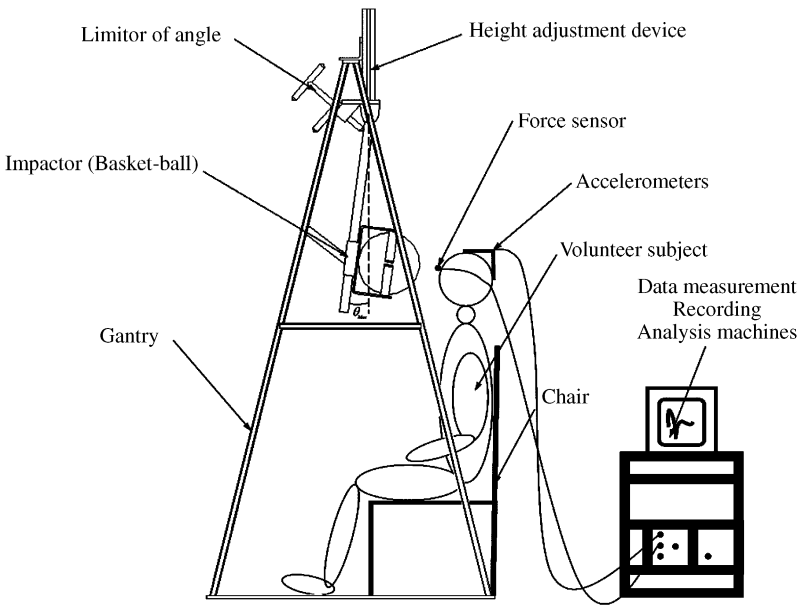

Fig. 1. Experimental test device for the modal analysis of the head–neck system.

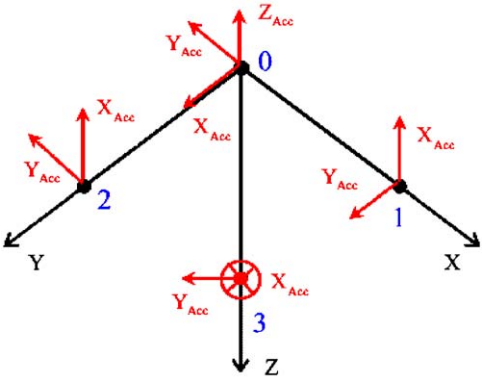

Fig. 2. The 3-2-2-2 configuration of nine accelerometers of the head.

Force and acceleration signals are digitized with a National Instrument (NI) data acquisition and signal conditioning machine PXI-1010 with a PXI-6070E 12 bit card. Signal acquisition is obtained with a LabView (NI) programme and data processing written to Matlab software. Antero-posterior linear accelerations are calculated at the vertex level (S point).

After impact, the transfer function between the force and S point acceleration is estimated in terms of apparent mass. Special attention was paid to noise management and checking the linearity, ergodicity and stationary nature of the signals.

In order to minimize noise associated with the digitizing effects, the standard normalized error is calculated by repeating each experiment ten times. The estimated transfer function and standard deviation are then calculated with their 95% confidence limits. The first step however involves confirming the linearity of the head–neck system by calculating the coherence function between the input force signal ($x(t)$) and the output acceleration ($y(t)$). The equation of the coherence function can be written as

$$\hat{\gamma}^2_{xy}(w) = \frac{\left|G_{YX}(w)\right|^2}{G_{YY}(w)G_{XX}(w)}, \tag{1}$$

where G_{XX}, G_{YY} and G_{XY} are the autospectrums and interspectrum of the signals obtained in the frequency domain [29].

The system is generally accepted to be linear if the coherence function remains between 0.9 and 1 in the frequency range analysed. The response signal contains not only the response due to the measured excitation, but also the response due to ambient random excitation. This typical measurement can therefore be characterized as having noise in the measured output signal. Using the principle of least squares to minimize the effect of noise at the output the best frequency response function (FRF) estimator is

$$\hat{H}(w) = \frac{G_{XY}(w)}{G_{XX}(w)} = \left|\hat{H}(w)\right| e^{-j\hat{\Phi}_1(w)}. \tag{2}$$

Under these conditions the errors associated with the amplitude and phase of the transfer function, respectively, are given by Eqs (3) and (4) and are illustrated in Fig. 3. Eq. (3) introduces

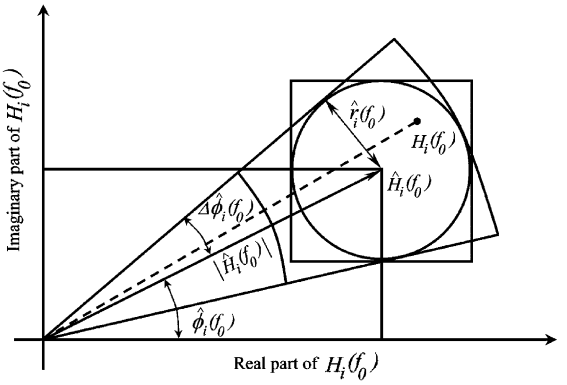

Fig. 3. Representation of the transfer function confidence interval.

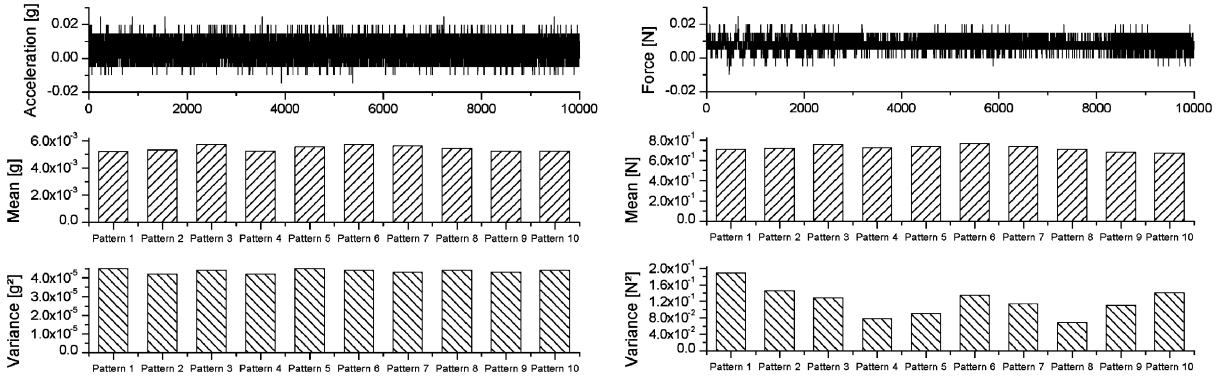

Fig. 4. Stationnarity cheking: Mean value of the noise and standard deviation for the two signals (acceleration left and force right).

the Fischer distribution $F_{2,n-2}$ with 2 and $n-2$ degrees of freedom [29]:

$$\hat{r}^2(w) = \frac{2}{n-2} F_{2,n-2}[1-\hat{\gamma}_{xy}(w)]\frac{G_{YY}(w)}{G_{XX}(w)}, \tag{3}$$

$$\Delta\hat{\Phi}(w) = \arcsin\left[\frac{\hat{r}(w)}{|\hat{H}(w)|}\right]. \tag{4}$$

Before carrying out the experiments, stationarity and ergodicity of the signals are also confirmed in order to apply the above principles. The signal is therefore recorded over ten seconds with a sampling rate of 1000 Hz using a 100 Hz filter without head movement. An average value for each pattern of 1000 samples is calculated for each channel, and it is assumed that if all of the average values are equal, the system is stationary [29]. The average values of noise relating to those signals remained almost constant, as did their standard deviation values. These are illustrated in Fig. 3. This demonstrates the stationary nature of the signals. Ergodicity was checked by comparing the statistic mean value with the probabilistic mean value (Fig. 4). Fig. 5

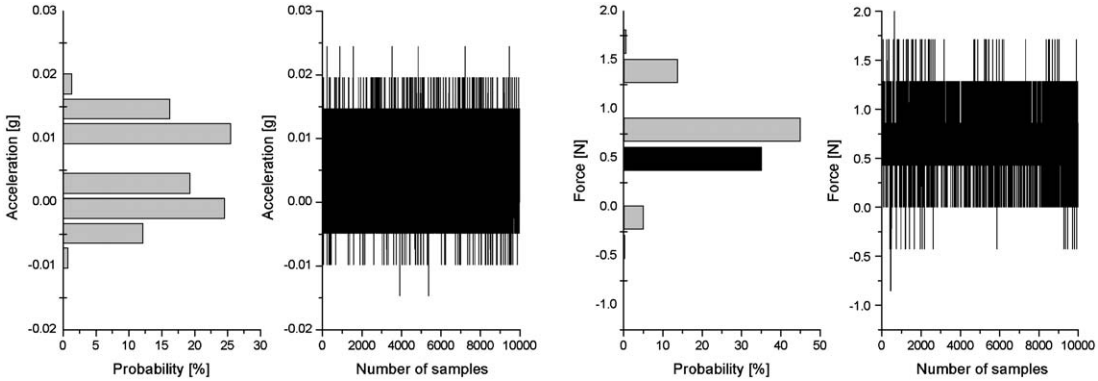

Mean		Accelerometric noise	Force noise
Temporal	$m_{temporal} = \frac{1}{N}\sum_{i=1}^{N} x(i)$	$m_{temporal} = 0,00543$	$m_{temporal} = 0,721$
Probabilitic	$m_{probabilité} = \sum_{k=1}^{Q} l(k).p(k)$	$m_{probabilité} = 0,00505$	$m_{probabilité} = 0,00724$

Fig. 5. Ergodicity checking: Temporal and probabilistic averages of both signals demonstrating ergodicity.

shows the mathematical expression of both means and the values of the force and acceleration signals.

This study focuses on frequency response of the head–neck system in the 0–20 Hz range. The recorded signal is conditioned with a 100 Hz Butterworth filter and covers a 5 s duration with a sample rate of 1000 Hz. It is important to record the signal over a long period of time in order to have sufficient information at low frequencies. Typical results of force and acceleration evolution in the temporal domain relating to the first volunteer subject (VS01) are plotted in Fig. 6.

The transfer function between force and acceleration was then calculated in terms of apparent mass using Eq. (2). The frequency diagram (amplitude and phase) of the apparent mass and the coherence function are shown in Fig. 7. The coherence between 0.9 and 1 at frequencies contained in the 0.7–30 Hz range (which gives the validation domain of the transfer function) confirms the linear behaviour of the head–neck system under study conditions.

This result obtained from ten recordings on one subject demonstrated a first natural frequency at 1.4 Hz, illustrated by a minimum amplitude of apparent mass and phase change from -180° to -32° with a -90° phase at 1.4 Hz. In addition, at 6 Hz, a second minimum amplitude value accompanied by phase shift demonstrates a second natural frequency, although not necessarily at this frequency because of damping. Ultimately, above 12 Hz, the head–neck system behaves as a single mass illustrated by a constant apparent mass amplitude. This is a typical result for a system with two degrees of freedom. The simplest model which can simulate this transfer function is therefore a two mass system connected with a set of springs and dashpots. This is provided by the classical two pivot neck model.

A single transfer function between acceleration at the vertex and the input force to the forehead cannot contain all of the information describing a system with two degrees of freedom. A second

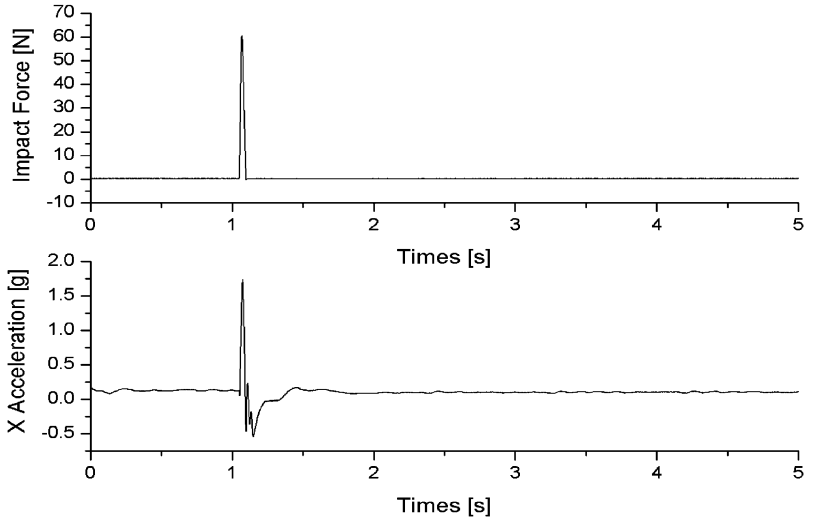

Fig. 6. Temporal evolution of applied force and linear acceleration response calculated at vertex level.

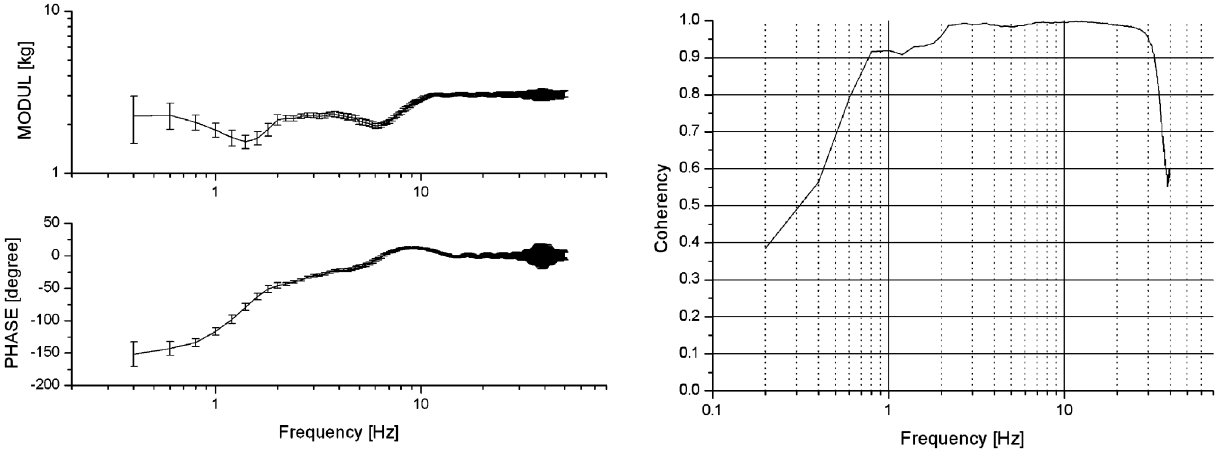

Fig. 7. Experimental apparent mass of the head–neck system with 95% confidence for the subject VS01 (on the left), and the coherence function associated (on the right).

transfer function is required to extract the mode shape relating to each natural frequency. The horizontal linear acceleration at the atlanto-occipital joint (O_H point) is chosen for this purpose and the transfer function between this parameter and the input force is determined in a similar way to the transfer function between S point acceleration and force (see Fig. 8).

The system's natural frequencies are extracted by plotting the real part of both transfer function at vertex and at the atlanto-occipital joint in terms of dynamic stiffness, according to Ewins [30]. This is illustrated in Fig. 9. Frequencies at the "half-power-points" (f_a and f_b) facilitated calculation of the natural frequencies f_r and the modal damping ratio η according

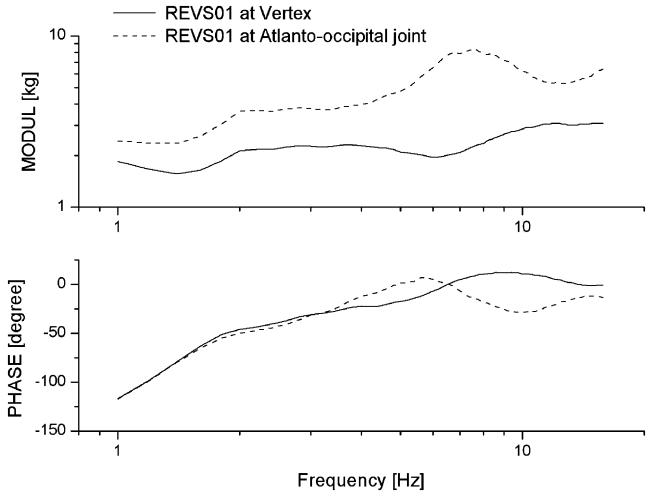

Fig. 8. Experimental Transfer functions recorded at the vertex and the atlanto-occipital joint in term of apparent mass.

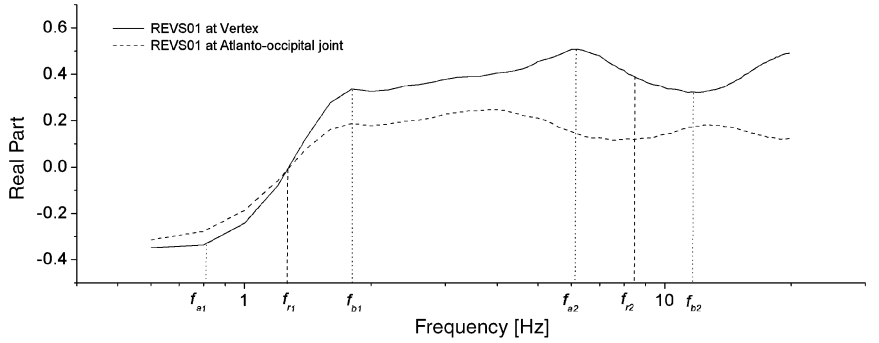

Fig. 9. Real part of both experimental transfer function between vertex acceleration and force and atlanto-occipital acceleration and force in terms of dynamic stiffness.

to the Eq. (5) (Ewins [30]).

$$\eta = \frac{f_b - f_a}{2f_r} \quad \text{and} \quad \begin{cases} f_a = f_r\sqrt{1-\eta} \\ f_b = f_r\sqrt{1+\eta} \end{cases} \text{ so } f_r^2 = \frac{f_a^2 + f_b^2}{2}. \tag{5}$$

The natural frequencies obtained with Eq. (5) are given in Table 1. The first mode occurs at 1.4 Hz where the apparent mass is at minimum amplitude whereas the second mode is located at 8.8 Hz, which does not correspond to the minimum apparent mass amplitude seen at 6 Hz. This difference is due to modal damping which is known to shift the natural frequency. The higher the natural frequency the stronger is the damping effect. Therefore, the first natural frequency is less affected by damping. The results are shown in Table 1.

Table 1
Experimental natural frequencies estimated on the relaxed volunteer subject VS01

Mode	f_a (Hz)	f_b (Hz)	f_r (Hz)	η
1	0.8	1.8	1.4	0.35
2	6	11	8.8	0.28

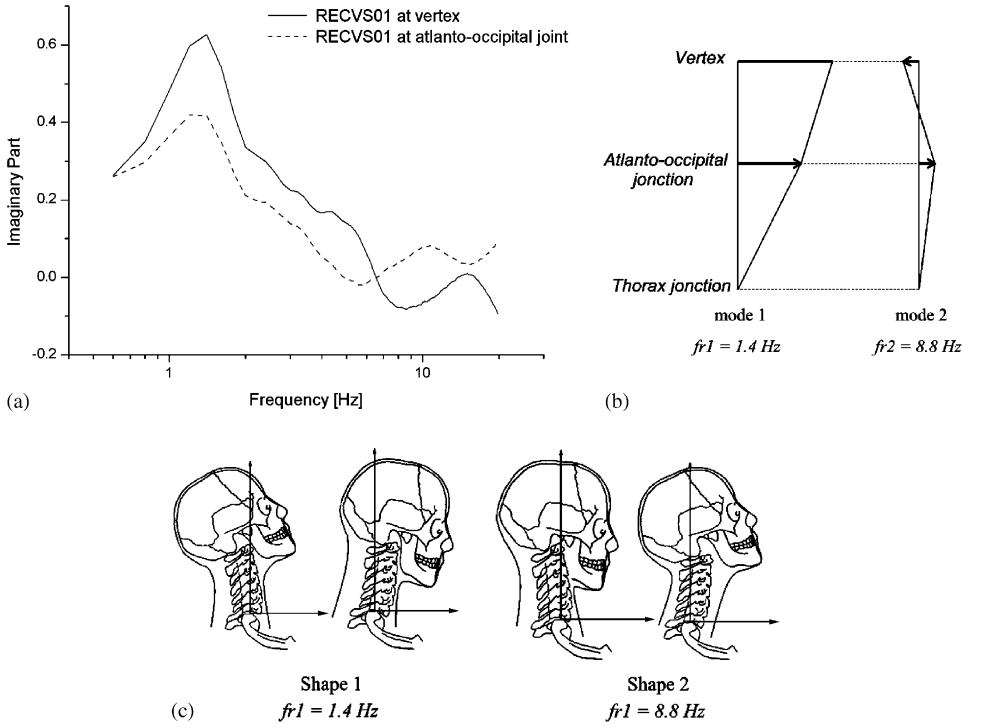

Fig. 10. Experimental deformed mode shapes obtained with eigenvectors extracted from the dynamic stiffness imaginary part.

The final stage in the experimental modal analysis of the first subject's head–neck system is mode shape. According to Ewins [30], the imaginary part of both transfer functions, i.e. at the vertex and at the atlanto-occipital joint, illustrated in Fig. 10, made it possible to estimate the Eigen vectors ψ_r. The imaginary part of both transfer functions are plotted in Fig. 10a. The value of the imaginary part of both transfer functions at each natural frequency defines the Eigen vectors shown in Fig. 10b. The mode shapes obtained are drawn in Fig. 10c where it can be clearly seen that the first mode at 1.4 Hz is an extension mode and the second mode at 8.8 Hz a retraction mode.

3. Inter-subject variability

Following the detailed analysis of an individual volunteer it is important to evaluate inter-subject variability of experimental apparent mass, natural frequencies and the mechanical

parameters relating to each subject under similar conditions. A total of five volunteers underwent the experiment described above. All of the subjects were male, of different weights and heights. The next four experimental apparent mass values between vertex acceleration and impulse force are shown in Fig. 11, together with their coherence function.

The coherence functions are close to 1 in the frequency range analysed which demonstrates the linear behaviour of the head–neck system under study conditions. It can also be seen that the amplitudes of apparent masses displayed two minima at 1.4 Hz and between 7 and 9 Hz.

The transfer functions of the five volunteers have been superimposed on the same diagram in Fig. 12 for comparison. Fig. 13 shows the average of the five transfer functions with their standard deviations.

All of the subjects display a similar frequency response, characterized by two natural frequencies: the first mode at 1.3 ± 0.1 Hz and the second mode at 8 ± 0.7 Hz. The recorded values of these frequencies are almost constant, as shown in Table 2: Experimental natural frequencies for the five volunteers and average value with standard deviation. The transfer function between

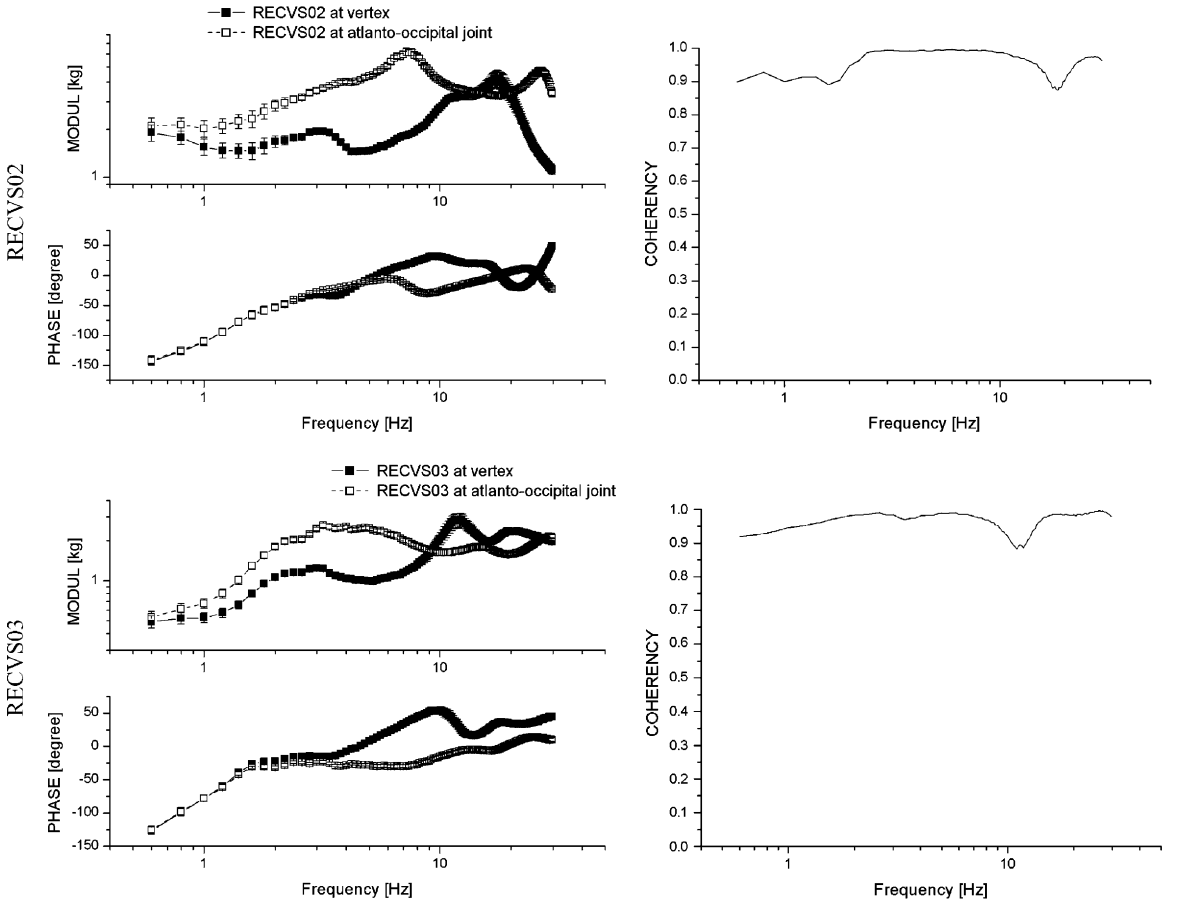

Fig. 11. Frequency diagram of the apparent mass between vertex acceleration and force and atlanto-occipital acceleration and force, and coherence functions relating to the four other volunteers.

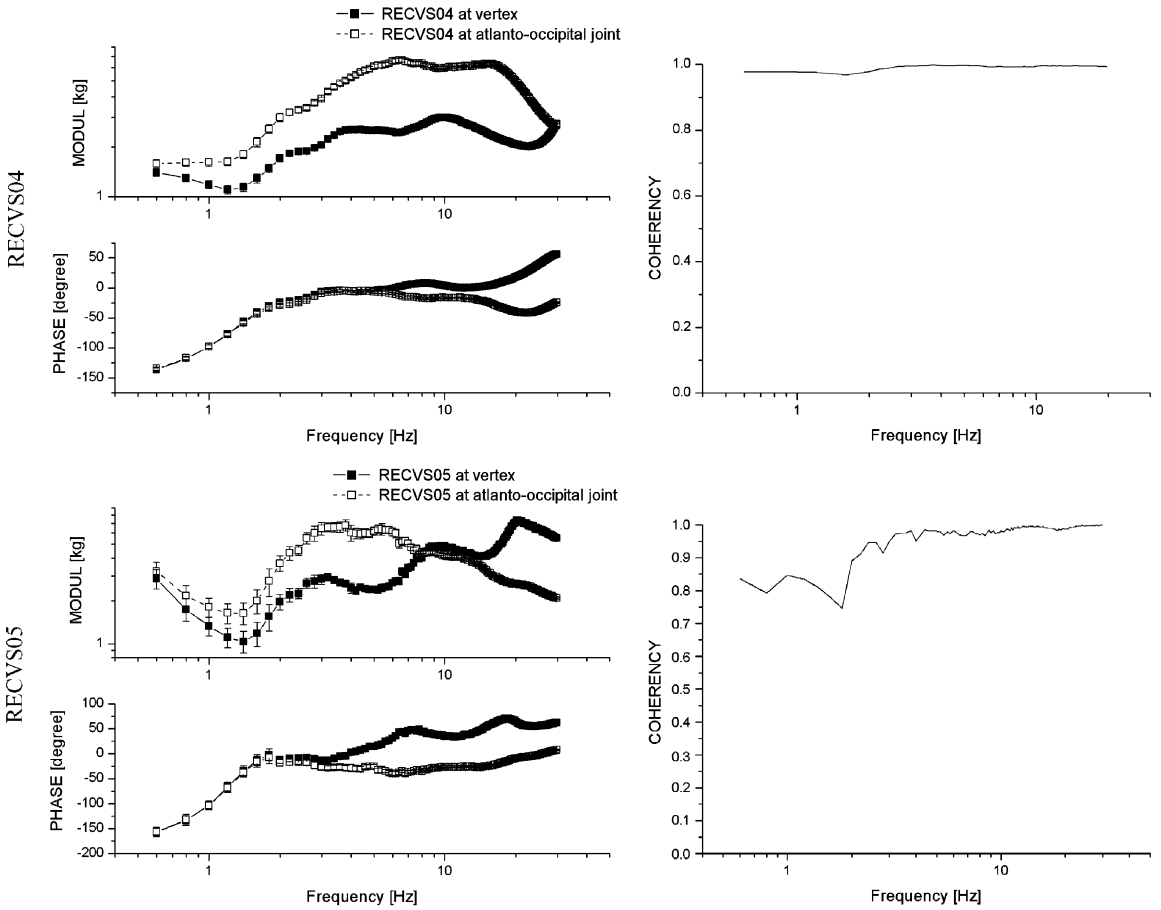

Fig. 11. (*Continued*)

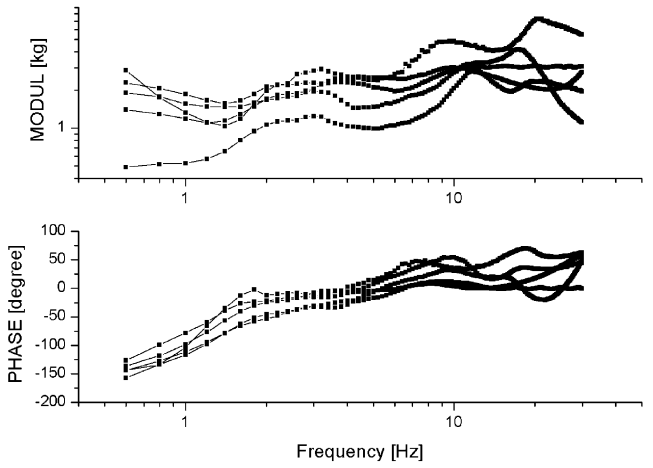

Fig. 12. Superimposition of the transfer functions between vertex acceleration and force for the five volunteers.

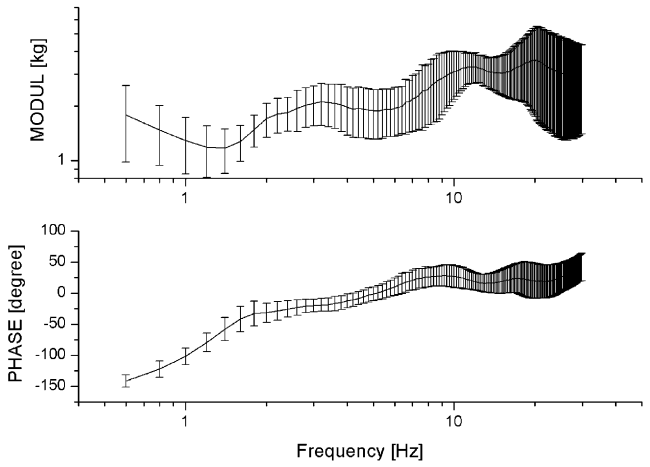

Fig. 13. Average of the five transfer functions between vertex acceleration and force and standard deviations.

Table 2
Experimental natural frequencies for the five volunteers and average value with standard deviation

Volunteer subject	f_{r1} (Hz)	f_{r2} (Hz)
VS01	1.4	8.8
VS02	1.4	8
VS03	1.4	7.8
VS04	1.3	8.4
VS05	1.2	7
Mean	1.34 ± 0.1	8 ± 0.7

atlanto-occipital joint and force was calculated for all subjects but are not shown. All clearly displayed the two mode shapes described in the previous section.

4. Lumped model and parameter identification

The two pivot head–neck model is not an original representation of the human neck. Both Bowman and Robbins and Wismans et al. [14,15] have suggested similar models, probably motivated by the fact that maximum mobility is seen at the upper and lower cervical column. Based on the experimental modal analysis, our approach has provided new insight into this model at two levels. The first is the model's parameter identification, superimposing experimental and theoretical transfer functions and the second concerns the model validation with respect to natural frequencies and the extracted mode shapes.

The model is shown in Fig. 14. Apart from the rigidity and damping value determined from identifying mechanical parameters, a number of anthropometric data must be captured. Direct

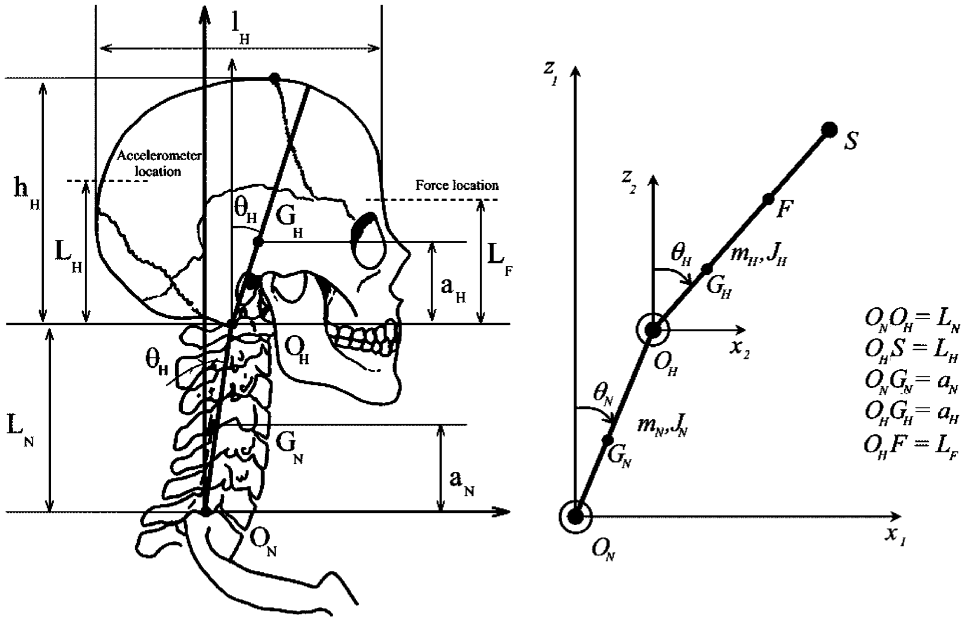

Fig. 14. Anatomic definition and Mathematical model of the head–neck system.

Table 3
Anthropometric data relating to the five volunteer subjects

	Age	Sex	Hight (m)	M (kg)	L_N (m)	a_N (m)	m_N (kg)	J_N (kg m^2)	L_F (m)	L_H (m)	a_H (m)	m_H (kg)	J_H (kg m^2)
VS01	26	M	1.93	75	0.13	0.065	1.7	0.0038	0.08	0.15	0.04	4.7	0.0209
VS02	42	M	1.65	55	0.10	0.05	1.1	0.0017	0.08	0.15	0.04	4.4	0.0191
VS03	25	M	1.91	95	0.12	0.06	2.3	0.0063	0.08	0.15	0.045	5.3	0.0263
VS04	34	M	1.78	75	0.12	0.06	1.7	0.0038	0.08	0.15	0.035	4.7	0.0209
VS05	48	M	1.71	64	0.11	0.055	1.2	0.0021	0.08	0.15	0.04	4.6	0.0209

measurement on the subject provides the geometrical parameters. The evaluation of masses and inertia is based on anatomical studies from the literature as described below.

For the head, mass was correlated with the circumference and weight of the volunteer by Clauser et al. [31]. Head inertia momentums were studied by McConville et al. [32] as a function of circumference, length and width of the volunteer's head. Finally, Walker et al. [33] positioned the head centre of mass a_H at 40% of the head height. Walker et al. also investigated neck mass and inertia by approximating it to a cylinder. Neck mass and the relevant moment of inertia are therefore given as a function of its dimensions, with the centre of mass located at 50% of neck height. All of the individual volunteer parameters are shown in Table 3.

The two pivot model is a double reversed physical pendulum of mass m_N and m_H respectively for the neck and the head. This is shown in Fig. 15. The quantities a_N and a_H are the distances from the mass centres to the corresponding pivoted points O_N and O_H, respectively. Let J_N and J_H be the moments of inertia of the pendulums with respect to the axis of rotation and ψ and θ be the degree of freedom of the model defined by: $\psi = \theta_H - \theta_N$ and $\theta = \theta_N$, respectively. Under the

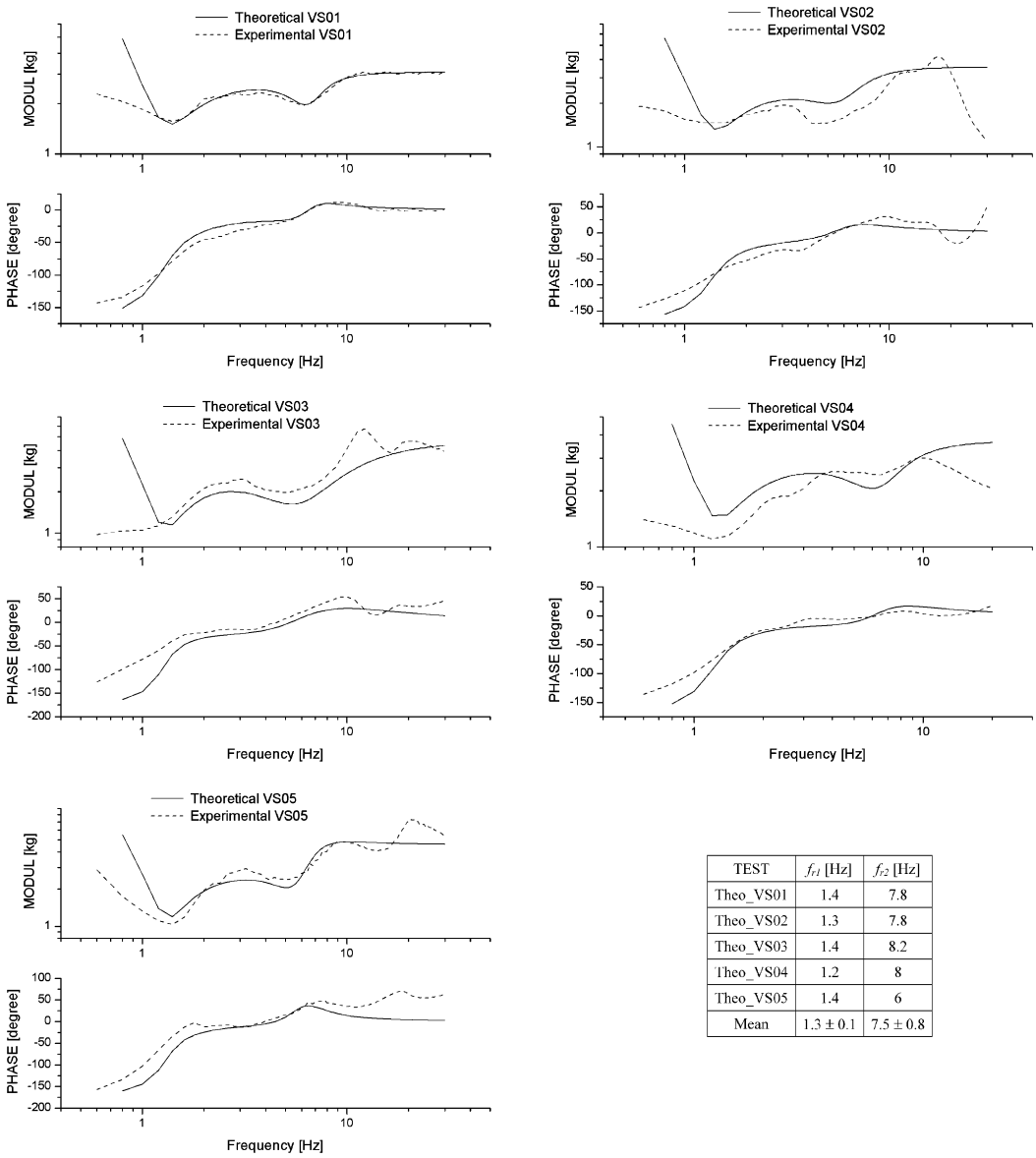

TEST	f_{r1} [Hz]	f_{r2} [Hz]
Theo_VS01	1.4	7.8
Theo_VS02	1.3	7.8
Theo_VS03	1.4	8.2
Theo_VS04	1.2	8
Theo_VS05	1.4	6
Mean	1.3 ± 0.1	7.5 ± 0.8

Fig. 15. Superimposition of theoretical and experimental apparent mass at vertex level for the five volunteer subjects and theoretical natural frequencies for the five models.

hypothesis of small displacements, consider the equations of motion:

$$\begin{aligned}&\left[J_H + m_H a_H^2\right]\ddot{\psi}(t) + c_H\dot{\psi}(t) + [k_H - m_H g a_H]\psi(t) - m_H g a_H\theta(t) + [J_H + m_H a_H(a_H + L_N)]\ddot{\theta}(t)\\ &= F(t)L_F\left[J_N + J_H + m_N a_N^2 + m_H L_N^2 + m_H a_H L_N\right]\ddot{\theta}(t) + c_N\dot{\theta}(t) + [k_N - g(m_N a_N + m_H a_H\\ &\quad + m_H L_N)]\theta(t) - m_H g a_H\psi(t) + [J_H + m_H a_H(a_H + L_N)]\ddot{\psi}(t) = F(t)(L_N + L_F),\end{aligned} \tag{7}$$

where (k_N,c_N) and (k_H,c_H) are the rigidity and damping corresponding to the pivoted points O_N and O_H, respectively, and $F(t)$ is the impulse force. In the frequency domain, this equation leads to Eq. (8):

$$\begin{vmatrix} jc_H w + K_H - M_\Psi w^2 & -\left[m_H g a_H + M_{\Psi\Theta} w^2\right] \\ -\left[m_H g a_H + \mathrm{M}_{\Psi\Theta} w^2\right] & jc_N w + K_N - M_\Theta w^2 \end{vmatrix} \begin{vmatrix} \Psi(jw) \\ \Theta(jw) \end{vmatrix} = \begin{vmatrix} F(jw)L_F \\ F(jw)(L_N + L_F) \end{vmatrix}, \tag{8}$$

where

$$\begin{aligned} K_N &= k_N - g(m_N a_N + m_H a_H + m_N L_N) \\ K_H &= k_H - m_H g a_H \end{aligned} \quad \text{and} \quad \begin{aligned} M_\Psi &= J_H + m_H a_H^2 \\ M_\Theta &= J_N + J_H + m_N a_N^2 + m_H(L_N + a_H) \\ M_{\Psi\Theta} &= J_H + m_H a_H^2 + m_H a_H L_N. \end{aligned} \tag{9}$$

The solution of this system is given by Eq. (10), which express the transfer function between the input force and the two degrees of freedom:

$$\begin{aligned} \Psi(jw) &= \frac{L_F[jc_N w + K_N - M_\Theta w^2] + (L_N + L_F)M_{\Psi\Theta} w^2}{[jc_H w + K_H - M_\Psi w^2][jc_N w + K_N - M_\Theta w^2] - [m_H g a_H + M_{\Psi\Theta} w^2]^2} = F(jw), \\ \Theta(jw) &= \frac{(L_N + L_F)[jc_H w + K_H - M_\Psi w^2] + L_F M_{\Psi\Theta} w^2}{[jc_H w + K_H - M_\Psi w^2][jc_N w + K_N - M_\Theta w^2] - [m_H g a_H + M_{\Psi\Theta} w^2]^2} = F(jw). \end{aligned} \tag{10}$$

These two equations finally describe our system in the frequency domain. However, in order to superimpose the experimental transfer functions onto the theoretical, we must now express the transfer function between input force and output acceleration at the vertex (S point in Fig. 14). This is achieved by Eq. (11) in terms of apparent mass:

$$M_{\mathrm{app}}(jw) = \frac{F(jw)}{\Gamma(jw)}$$

with

$$\delta(jw) = L_H\Psi(jw) + (L_N + L_H)\Theta(jw)$$

and

$$\Gamma(jw) = -w^2\delta(jw). \tag{11}$$

As for the experimental modal analysis, two transfer functions are needed to extract the deformed mode shapes relating to each identified natural frequency. The expression of three transfer functions in terms of dynamic stiffness is given in Eq. (12), one for the S point directly

Table 4
Optimized mechanical parameters of the neck model for the five volunteer subjects and for the "Mean subject"

TEST	k_N (Nm/rad)	c_N (Nm s/rad)	k_H (Nm/rad)	c_H (Nm s/rad)
Theo_VS01	20	0.8	18	0.1
Theo_VS02	16	1.1	12	0.1
Theo_VS03	13	0.3	10	0.1
Theo_VS04	20	0.7	18	0.2
Theo_VS05	19	0.6	11	0.05
Mean	17 ± 3	0.7 ± 0.3	13.8 ± 4	0.11 ± 0.05

derived from Eq. (11), another for the O_H point based on a similar method and finally the zero function at the embedded point O_N.

$$\begin{array}{ll} \text{Spatial point} & \text{Dynamic stiffness} \\ O_N & \alpha_{O_N}^{-1} = 0 \\ O_H & \alpha_{O_H}^{-1} = \dfrac{L_N \Theta(jw)}{F(jw)} \\ S & \alpha_S^{-1} = \dfrac{L_H \Psi(jw) + (L_N + L_H)\Theta(jw)}{F(jw)}. \end{array} \tag{12}$$

We now have all the information required to proceed to identify the mechanical parameters by superimposing the experimental and theoretical apparent mass transfer function between force and vertex acceleration. This was achieved by an optimization method using minimization of the square distance value. Fig. 15 shows the optimized theoretical apparent mass superimposed on the experimental apparent mass for the five volunteers. Theoretical natural frequencies are obtained at 1.3 ± 0.1 and 7.5 ± 0.8 Hz versus 1.3 ± 0.1 and 8 ± 0.7 Hz at the experimental level. Table 4 shows the model's mechanical parameters obtained by this optimization procedure for the five subjects together with their mean values and standard deviations, defining a "mean subject".

The model's realistic mode shapes were confirmed by plotting the imaginary part of the dynamic stiffness at S, O_H and O_N for both the analytical model and volunteers. Similar changes in the imaginary parts of transfer function confirmed that neck extension motion and head retraction were associated with the first and second natural frequencies respectively in all of the volunteers.

5. Modal evaluation of crash test dummy necks

Based on the new biomechanical characterization of the human head–neck system in vivo described above, this section evaluates the biofidelity of existing crash test dummies in the frequency domain. As for the volunteers, dummy head acceleration was measured using nine accelerometers in order to calculate the linear component of head acceleration at any point. Impulse force was recorded using the same force sensor as in the volunteers. A total of four dummy necks were evaluated in this study; the Hybrid III-neck which is a commonly used crash

dummy under frontal and rear end impact, and three rear-end dummy prototypes, the TRID, the BIORID II and the RID2 v0.0.

Hybrid III is a well-known frontal impact dummy extensively used as standard all over the world. It is also sometimes used for rear impact. This dummy was developed by General Motors and was accepted as a standard by NHTSA in 1986. The original neck of Hybrid III consists of a stack of aluminium discs moulded by rubber. The lower and higher plates are connected by a cable, which has an adjustable tension. This dummy neck is largely recognized to be too stiff and poorly reproduces the human head kinematics under rear impact. It was found in the 1980s that existing dummies exhibited different head rotation to that of human volunteers, particularly under moderate rear impact [9,34–36]. In 1992, Svensson and Lövsund [37] developed a new dummy neck with improved kinematic responses of the dummy in terms of head rotation although further modifications were also needed to reproduce translation of the head. After several dummy versions, a flexible vertebral column has now been added to the neck to reproduce T1 rotation accurately. This new rear impact dummy prototype is called the BioRID P3 [4]. BioRID II is the commercial version of BioRID P3. During the same period, Thunnissen et al. [38] developed another rear impact dummy neck prototype called the TRID-neck, used in combination with the Hybrid III dummy. Its general construction was similar to that of the BioRID P3 neck although it had a reduced number of discs representing the cervical vertebrae. Extensive validations have been conducted against new volunteer tests in the temporal domain and response reproducibility has been improved. New modifications have however been proposed within the context of the EU project ''Whiplash'' project started in 1997 leading to the RID2 v0.0 dummy in 2002. The new neck of this dummy has 7 aluminium discs connected to a central cable and external cables, which simulate muscle action. Rubber blocks inserted between the discs in the rear and lateral positions are specifically designed to adjust local stiffness of the cervical column.

The experimental transfer function between frontal force and vertex acceleration are plotted against apparent mass in Fig. 16 for the four crash dummies tested. In this figure, each dummy response is superimposed on the mean volunteer response for the biofidelity evaluation.

Whilst the inertial behaviour at high frequencies is realistic for the neck of the original Hybrid III dummy (Fig. 16a), the first recorded natural frequency appears at 5.5 Hz and after this extension mode, no retraction mode is seen in the 0–20 Hz frequency range. This result illustrates an excessively rigid extension mode (5.5 Hz) compared to the extension mode in vivo of 1.3 ± 0.1 Hz. It can be seen in Fig. 16b that the TRID-neck produces only a slightly different response compared to the original Hybrid III neck, and only reproduces the extension mode. An improvement was however obtained with a first natural frequency at 4.5 Hz compared to 5.5 Hz for the original Hybrid III neck. BioRID II's experimental apparent mass in Fig. 16c shows a significant improvement in neck flexibility, as its first natural frequency is reduced to 2.3 Hz. Compared to the human neck, it can be concluded that this dummy neck is still too stiff and that its damping ratio is far too low. The apparent mass amplitude plotted in this figure does not allow a second mode to be defined. The RID2 v0.0 exhibits very similar mechanical behaviour to the BIORID II. Its experimental apparent mass is plotted against the volunteers' response in Fig. 16d. The first mode (extension) is at 2.7 Hz, which is still too high compared to the volunteers (1.3 ± 0.1 Hz) although in this case improved damping is seen. Contrary to BioRID II, a second mode is clearly defined around 14 Hz (compared to 8 ± 0.7 Hz for the volunteers). However, this illustrates excessively rigid behaviour for the retraction mode.

The natural frequencies of the two new rear impact dummy prototypes are close to those of the human volunteers shown by the detailed analysis of modal behaviour. The damping ratio and mode shapes were extracted using the method described for human beings. The real part of dynamic stiffness for the BioRID II and RID2 v0.0 at vertex level are shown in Fig. 17a and b. In addition, for the purposes of illustrating mode shapes, Fig. 18a and b show the imaginary part of dynamic stiffness at both vertex and atlanto-occipital joint levels for both rear impact dummies.

The BioRID II (Figs. 18a and 19a) clearly displays only one natural frequency, at 2.3 Hz, corresponding to neck extension as illustrated in Fig. 19a. The damping ratio for this mode is 0.26, compared to 0.4 for the volunteers. It may be concluded that the BioRID II is slightly too stiff, that its extension mode is insufficiently dampened and that there is no retraction mode at all.

A very similar conclusion is drawn for the RID2 dummy neck when the first (extension) mode is examined, as shown in Fig. 18b. However, this dummy neck prototype displays a second mode at 14 Hz with a damping ratio of 0.2 (Fig. 17b) associated with a retraction mode shape as seen in

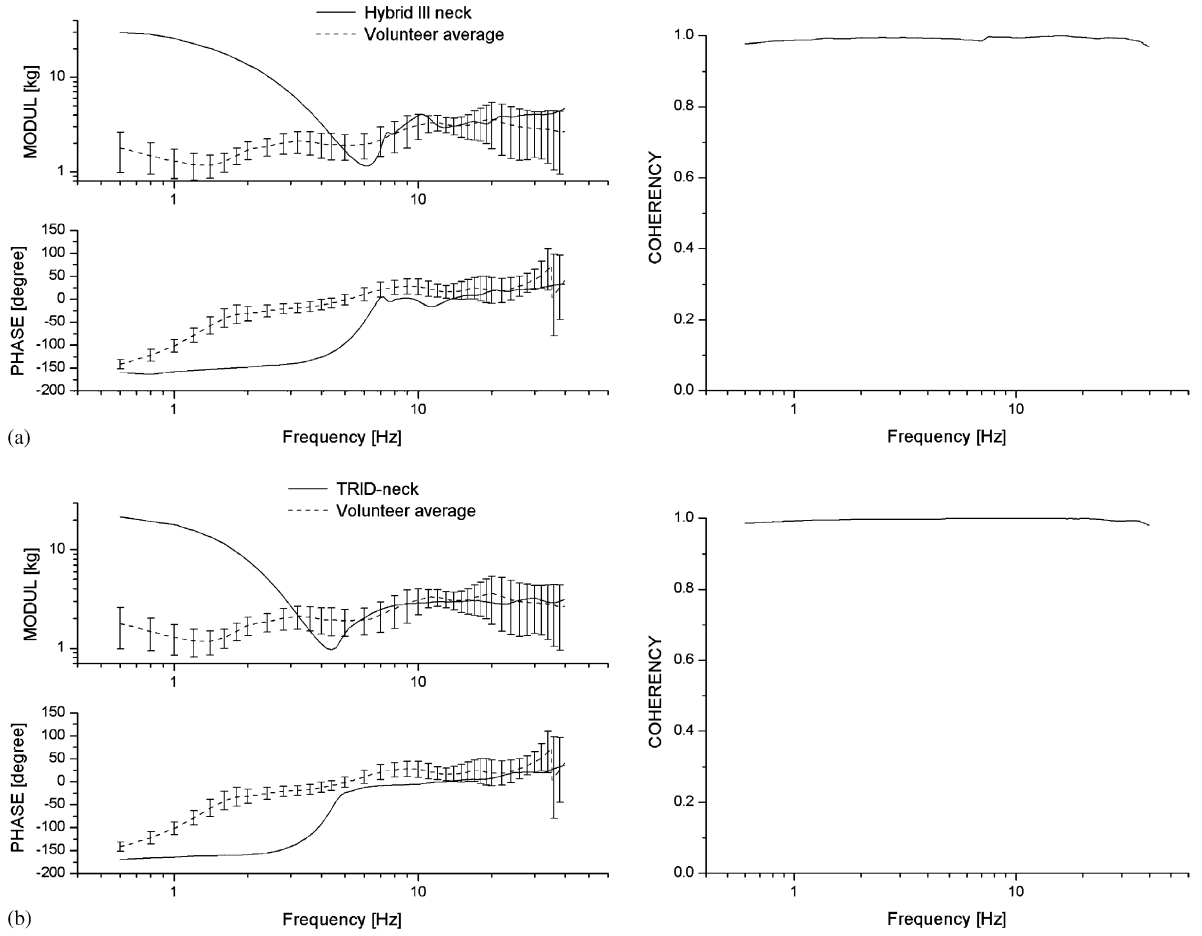

Fig. 16. Apparent mass between vertex acceleration and force with 95% of confidence (left) and the coherence functions (right) for (a) hybrid III original neck, (b) TRID-neck, (c) BioRID II neck, (d) RID2 v0.0 neck.

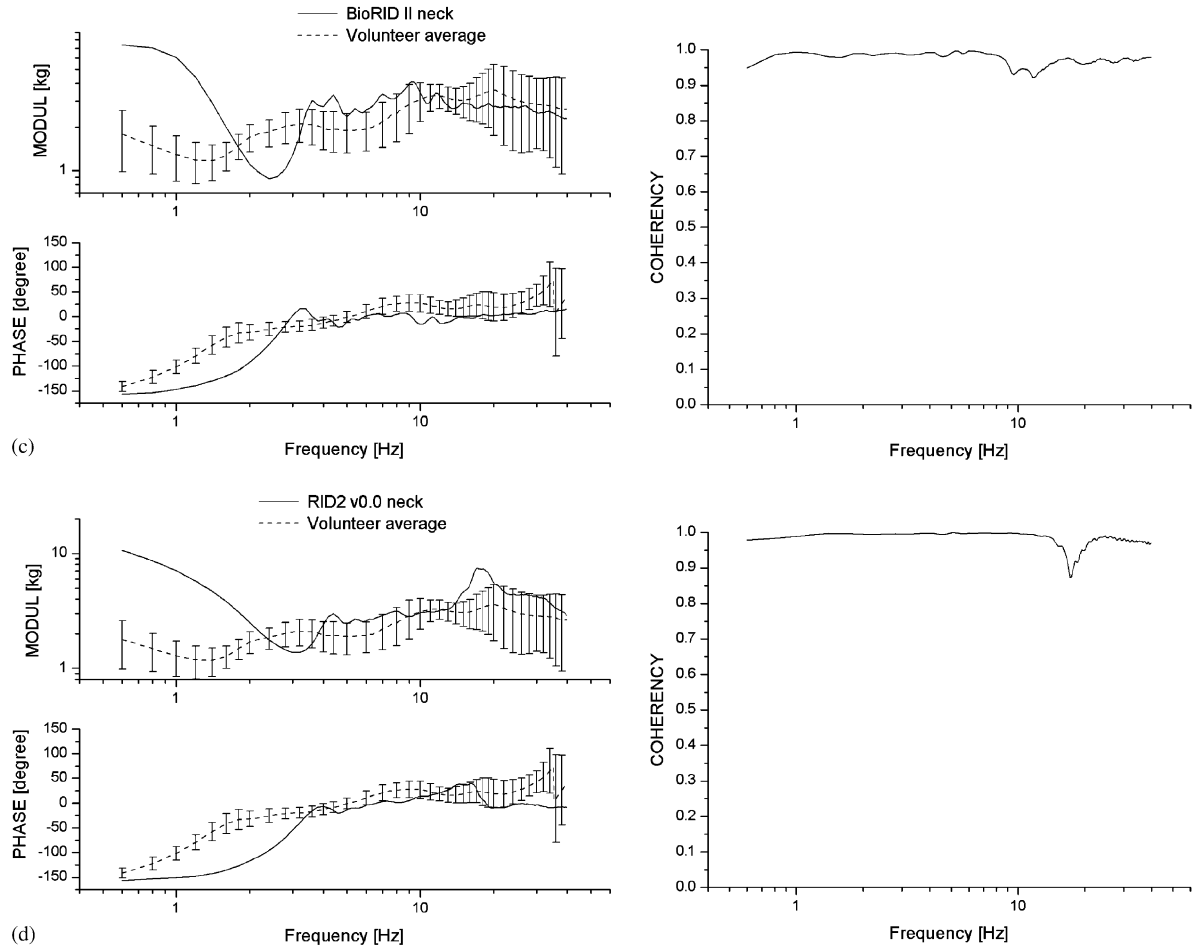

Fig. 16. (*Continued*)

human beings. This is illustrated in Fig. 18b. A main limitation of this dummy neck therefore is excessively weak damping and, in particular, a retraction mode which is far too rigid.

6. Discussion

The main methodological question is the assumption of linearity arising from the definition of transfer function and also the low impact energy involved in the experimental impact. It is important therefore to remember that the methodology is well designed to describe neck behaviour in low energy impact or before nonlinearity due to saturation (hyperextension of ligaments, bone contact, muscle activity) occurs. It is questionable whether the neck really exhibits nonlinear behaviour under low speed rear impact. Bogduk et al. [18] as Mc Connell et al. [35], Yoganandan et al. [39] and Matsushita et al. [40] have stated that the head does not rotate beyond

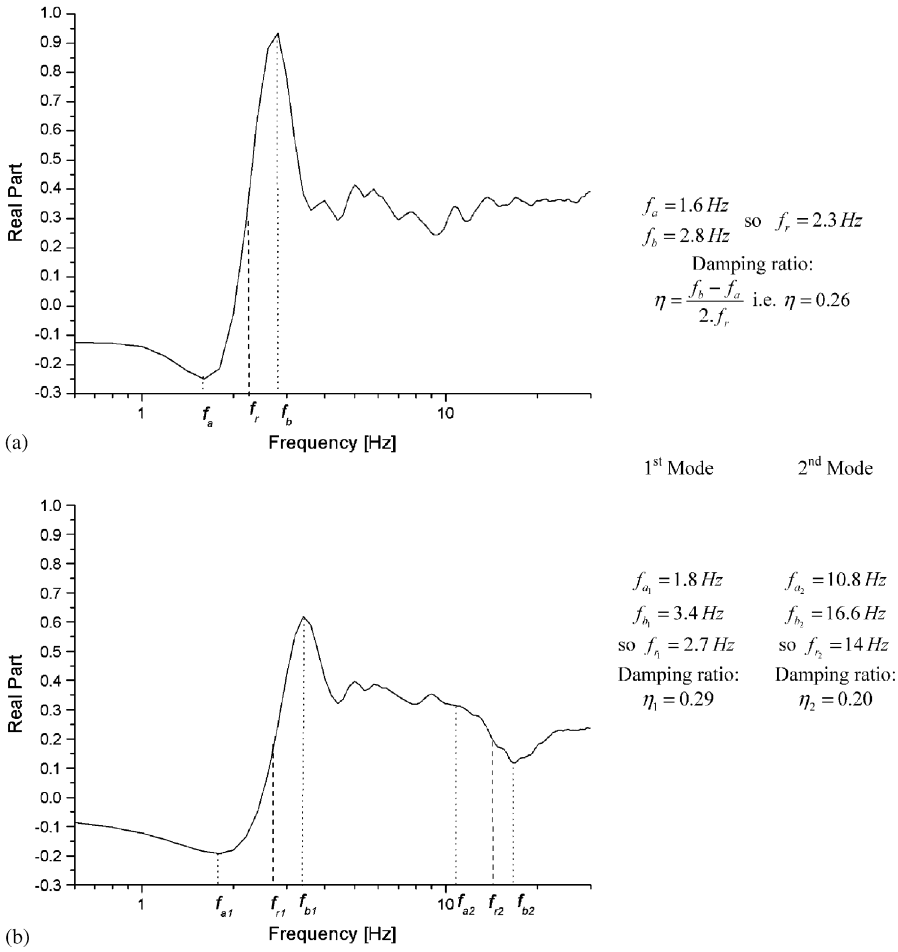

Fig. 17. Real part of the dynamic stiffness at vertex level for (a) BioRID II and (b) RID 2.

physiological limits. In the real world, accident injuries are also often seen even when the head rest is present, under low energy, showing that it can occur early after impact before extension of the head takes place and probably before nonlinear behaviour appears. This illustrates that injuries may occur under low displacement conditions.

On the other hand, linear behaviour has been confirmed in our experiments by the coherence function, which remains between 0.9 and 1. The results illustrate the importance of mass distribution and damped elastic properties at the beginning of the motion. Resonance frequencies and mode shapes provide initialization for the dynamic deformation that may eventually continue until nonlinearity appears in case of energetic impact. The definition of mode shape hinders our understanding of the mechanisms of injury even if movements are restricted to small deformations. In our case, the extracted modal characteristics of the neck represent "Eigen" mechanical data for the head–neck system in the sagittal plane whatever the loading conditions. New validation parameters are therefore determined for a model, restricted to low energy impacts,

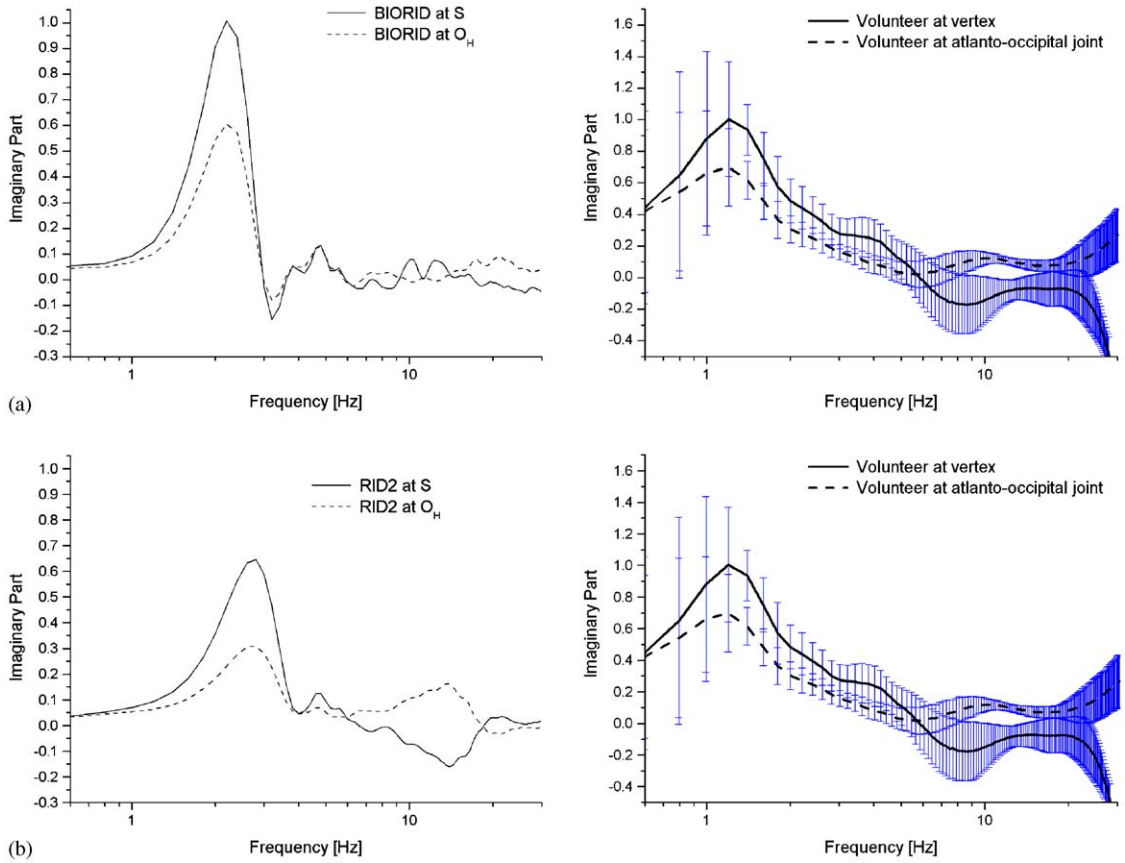

Fig. 18. Superimposition of the imaginary part of the dynamic stiffness at vertex level (S) and and atlanto-occipital junction (O_H) for dummy neck (left) and for the human volunteer average (right): (a) BioRID and (b) RID2.

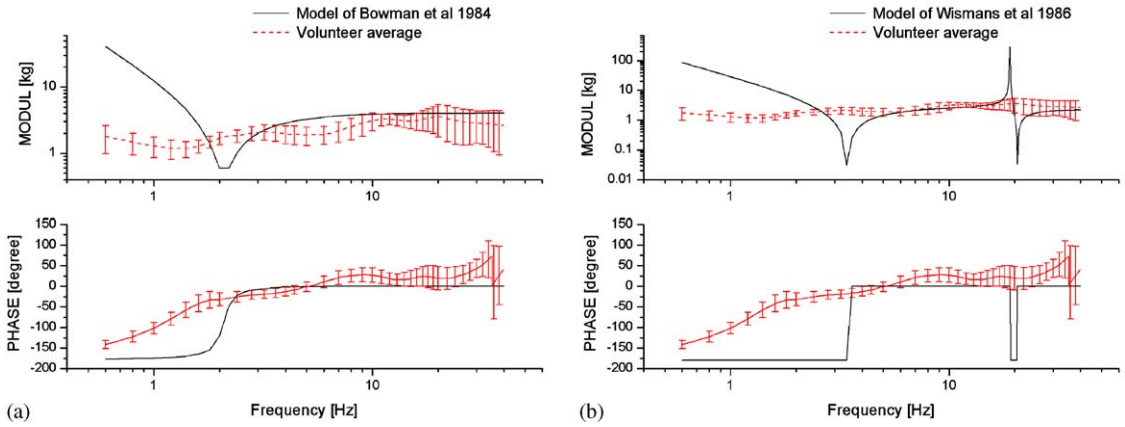

Fig. 19. Superimposition of the experimental apparent mass function of the volunteer with the apparent mass calculated or recorded with: Bowmann and Robbins [14] and Wismans et al.'s [15] model.

remaining in the sagittal plane. On the other hand the response of the temporal model will clearly depend on loading conditions such as location of head impact, impact force time history or inertial head loading due to first thoracic vertebra acceleration in the antero-posterior direction. This loading condition is the link with whiplash analysis, which is examined in this study. The results of the modal analysis however can be used for air bag induced frontal head loading investigation and in the context of any low energy sagittal head–neck loading.

The experimental vibration study under impulse condition for a first volunteer led to the identification of two natural frequencies at 1.4 and 8.8 Hz associated with two separate deformation mode shapes: neck extension and head translation, respectively. For a given volunteer, management of subject noise enabled a maximum standard deviation of 10% to be obtained for apparent mass and accuracy of ± 0.1 Hz for the natural frequencies. In order to evaluate the influence of inter-individual differences of head–neck modal behaviour, a total of five human male subjects were investigated. All of these displayed two natural frequencies at 1.3 ± 0.1 and 8 ± 0.7 Hz, respectively, associated with extension and retraction motion. The very similar modal behaviour of human subjects of quite different sizes and masses implies different rigidity and damping parameters, demonstrating that each subject has his/her own mechanical parameters, which in combination with inertial properties, lead to a given modal behaviour as found in this study, producing the overall result. It should be noted however that this study is restricted to relaxed human males excluding any muscle effect and with no investigation of females. The linearity assumption also excludes severe rear impact analysis with major neck extension and investigation of tolerance limits.

Extracted deformation modes have often been reported qualitatively in the literature, when volunteers were investigated in the temporal domain under rear impact condition. It has been reported that the retraction appears "a few milliseconds" before neck extension [16,20,23,41,42]. These findings are consistent with this modal analysis, although to our knowledge no study has clearly defined the conditions under which this retraction mode does or does not appear. This study leads us to the conclusion that the retraction mode is only excited if energy is introduced into the system above 8 Hz. This applies only if the impact duration is sufficiently short or if high loading ramps exist within the loading function. This is in complete agreement with Nightingale's findings following investigation of the neck under vertical loading with a multibody model restricted to the temporal domain [43]. The main result was that faster loading rates were associated with high-order buckling modes. In addition, these authors reported that injury mechanisms might be substantially changed by loading rates as inertial effects may influence whether or not the cervical spine fails in compression mode, or in bending mode in their case. In terms of modal analysis this statement simply becomes "if a natural frequency and its mode shape is excited, the related injury mechanism is potentially present". This study also therefore provides new insight into mechanisms of injury affecting the upper and lower cervical column following rear end impact.

The apparent mass results in this study led to a proposal for a two pivot lumped head–neck model as suggested around twenty years ago. Identification of the parameters of this model using an optimization method in the frequency domain led to rigidities of the model almost one tenth of those proposed by Bowmann and Robbins and Wismans et al. [14,15]. The frequency responses of this model have been investigated in the present study and are superimposed on the experimental data in Figs. 19a and b. These curves clearly illustrate that previous models satisfactorily

reproduce the extension mode close to 1.4 Hz but that the retraction mode is poorly reproduced (20 Hz compared 8.8 Hz in the experiment).

With respect to evaluating crash test dummy necks, the methodology proposed demonstrates a clear improvement in the neck extension behaviour of both dummy neck prototypes, as shown in the temporal domain. Prasad et al. [8] however reported exaggerated oscillations and a peak head extension time of approximately 50 ms shorter in the RID2 than in volunteers. These findings are confirmed in this study, demonstrating a first natural frequency, which remains excessively high and excessively low damping of this dummy neck. Prasad's study also showed that the head acceleration response in the rear impact dummy was shifted about 25 ms earlier in time compared to the human body. The second finding can be explained in our analysis by an excessively high second natural frequency of the dummy neck. Reproduction of head translation early after impact is undoubtedly still difficult to assess against the volunteer response in the time domain. This is a continuing field of investigation in the literature.

7. Conclusion

An experimental and theoretical modal analysis of the human head–neck system under frontal head impact, simulating low speed rear-end impact motion, has been successfully constructed and has produced new results:

- For the human head–neck system in vivo the extracted modal characteristics consist of a first natural frequency at 1.3 ± 0.1 Hz associated with neck extension and a second mode at 8 ± 0.7 Hz associated with head translation or neck retraction.
- This data set represents new validation parameters in the frequency domain suitable for dummy evaluation under moderate rear impact as well as the possibility to identify lumped model parameters.

By experimentally recording the apparent mass of dummy head–neck systems under the same experimental conditions as the volunteer subjects, we have been able to compare human and dummy frequency response functions and to evaluate their biofidelity against parameters in the frequency domain. The following conclusions can be drawn from this investigation:

- Hybrid III and TRID exhibits only one natural frequency at 5.5 and 4.5 Hz, respectively, associated with neck extension, which demonstrates their neck to be too rigid. Neck retraction mode was not seen.
- BioRID displays improved neck extension mode at 2.3 Hz. The retraction mode however is not reproduced in this prototype.
- RID2 also has a realistic extension mode even if slightly too stiff. In addition this neck prototype displays a retraction mode, although this degree of freedom is still far too stiff.

BioRID and RID2 are the most biofaithful rear impact dummies of the samples tested. Improvements are however needed to more closely reproduce the extension mode and to set the retraction mode at a realistic natural frequency.

To the authors' knowledge this is the first time that modal characteristics of the human head–neck system have been obtained. The results have led to a new methodology for dummy evaluation and provide new insight into injury mechanisms given that if a natural frequency and its mode shape are excited, there is a potential related injury mechanism present. Impact characteristics in the frequency domain or neck loading rate should therefore be managed to avoid a given neck deformation mode. This opens new possibilities for evaluation and optimization of protective systems. Consequently, we might be able to abolish or reduce transmissibility of seat to occupant between 6 and 10 Hz in order to avoid the neck retraction mode.

Acknowledgements

The authors wish to thank the French government for the support in the context of PREDIT program no. 00A008601.

References

[1] T.J. Szabo, D.P. Voss, J.B. Welcher, Influence of seat foam and geometrical properties on BioRID P3 kinematic response to rear impacts, presented at *IRCOBI Conference*, Munich, Germany, 2002.

[2] T.J. Szabo, J.B. Welcher, Human subject kinematics and electromyographic activity during low speed rear impacts, presented at *40th Stapp Car Crash Conference*, 1996.

[3] J.K. Foster, J.O. Kortge, M.J. Wolanin, Hybrid III—a biomechanically based crash test dummy, presented at *21st Stapp Car Crash Conference*, 1977.

[4] J. Davidsoon, *BioRID II Final Report*, Crash Safety Division, Departement of Machine and Vehicle Design, Chalmers University of Technology, Göteborg, Sweden, 1999.

[5] H. Cappon, M. Philippens, V. Ratingen, J. Wismans, Development and evaluation of a new rear-impact crash dummy, the RID2, *45th Stapp Car Crash Conference*, vol. 45, 2001, pp. 225–238.

[6] J. Davidsson, A. Flogård, P. Lövsund, M.Y. Svensson, BioRID P3—Design and Performance Compared to Hybrid III and Volunteers in rear Impacts at $V = 7$ km/h, presented at *43rd Stapp Car Crash Conference*, San Diego, California, 1999.

[7] J. Davidsson, P. Lövsund, K. Ono, M. Svensson, S. Inami, A comparison between volunteer, BioRID P3 and Hybrid III performance in rear impact, presented at *IRCOBI Conference*, Bron, France, 1999.

[8] P. Prasad, A. Kim, D.P.V. Weerappuli, Biofidelity of anthropomorphic test devices for rear impact, presented at *41th Stapp Car Crash Conference*, 1997.

[9] M.R. Seemann, W.H. Muzzy, L.S. Lustick, Comparison of human and Hybrid III head and neck response, presented at *30th Stapp Car Crash Conference*, 1986.

[10] G.P. Siegmund, B.E. Heinrichs, J.M. Lawrence, M. Philippens, Kinetic and kinematic responses of the RID2a, Hybrid III and Human Volunteers in low-speed rear-end collisions, presented at *45th Stapp Car Crash Conference*, 2001.

[11] T. Ishikawa, N. Okano, K. Ishikura, An evaluation of prototype seat using Biorid-P3 and Hybrid III with TRID neck, presented at *IRCOBI Conference*, Montpellier, France, 2000.

[12] A. Eichberger, B. Geigl, A. Moser, B. Fachbach, H. Steffan, W. Hell, K. Langwieder, Comparison of different car seats regarding head–neck kinematics of volunteers during rear end impact, presented at *IRCOBI Conference*, Dublin, Ireland, 1996.

[13] M. Svensson, P. Lövsund, Y. Håland, S. Larsson, The influence of seat-back and head-restraint properties on the head–neck motion during rear-impact, presented at *IRCOBI Conference*, Eindhoven, Netherlands, 1993.

[14] B.M. Bowman, D.H. Robbins, Parameter study of biomechanical quantities in analytical neck models, presented at *16th Stapp Car Crash Conference*, 1972.
[15] J. Wismans, H. Van Oorschot, H.J. Woltring, Omni-directional human head–neck response, presented at *30th Stapp Car Crash Conference*, 1986.
[16] Y.-C. Deng, W. Goldsmith, Response of a human head/neck/upper-torso replica to dynamic loading-II. Analytical/numerical model, *Journal of Biomechanics* 20 (1987) 487–497.
[17] M. De Jager, *Mathematical Head–Neck Models for Acceleration Impacts*, University of Technology, Eindhoven, 1996.
[18] N. Bogduk, N. Yoganandan, Biomechanics of the cervical spine—part 3: minor injuries, *Clinical Biomechanics* 16 (2001) 267–275.
[19] F. Dauvilliers, F. Bendjellal, M. Weiss, F. Lavaste, C. Tarrière, Development of a finite element model of the neck, presented at *38th Stapp Car Crash Conference*, 1994.
[20] M. Kleinberger, Application of finite element techniques to study of cervical spine mechanics, presented at *37th Stapp Car Crash Conference*, 1993.
[21] K. Yang, F. Zhu, F. Luan, L. Zhao, P.C. Begemen, Development of a finit element model of the human neck, presented at *42nd Stapp Car Crash Conference*, 1998.
[22] Golinski, *3D-Dynamic Modeling of the Human Cervical Spine in Whiplash Situations*, Nottingham University, Nottingham, 2000.
[23] K. Ono, K. Kaneoka, Motion analysis of human cervical vertebrae during low speed rear impacts by the simulated sled, presented at *IRCOBI Conference*, Hannover, Germany, 1997.
[24] K. Ono, K. Kaneoka, E.A. Sun, E.G. Takhounts, R.H. Eppinger, Biomechanical response of human cervical spine to direct loading of the head, presented at *IRCOBI Conference*, Isle of Man, UK, 2001.
[25] V.R. Hodgson, E.S. Gurdjian, L.M. Thomas, Determination of response characteristics of the head when impacting another body, with emphasis on mechanical impedance techniques, presented at *11st Stapp Car Crash Conference*, 1967.
[26] R.L. Stalnaker, J.L. Fagel, Driving point impedance characteristics of the head, *Journal of Biomechanics* 4 (1971) 127–139.
[27] R. Willinger, D. Cesari, Evidence of cerebral movement at impact through mechanical impedance methods, presented at *IRCOBI Conference*, Bron, France, 1990.
[28] S. Kitazaki, M.J. Griffin, Resonance behaviour of the seated human body and effects of posture, *Journal of Biomechanics* 31 (1998) 143–149.
[29] J.S. Bendat, A.G. Piersol, *Random Data: Analysis and measurement procedure*, Wiley-Interscience, New York, 1971.
[30] D.J. Ewins, *Modal Testing: Theory and Practice*, Research Studies Press Ltd., Tuanton, Somerset, England, 1984.
[31] C.E. Clauser, J.T. McConville, J.W. Young, Weight, volume and center of mass of segments of the human body, Wright Patterson Air Force Base, Ohio AMRL-TR-69–70, 1969.
[32] J.T. McConville, T.D. Churchill, I. Kaleps, C.E. Clauser, J. Cuzzi, Anthropometric relationships of body and body segment moments of inertia, Wright Patterson Air Force Base, Ohio AFAMRL-80–119, 1980.
[33] L.B. Walker, E.H. Harris, U.R. Pontius, Mass, volume, center of mass, and mass moment of inertia of head and neck of human body, presented at *17th Stapp Car Crash Conference*, 1973.
[34] Y.-C. Deng, Anthropomorphic dummy neck modelling and injury considerations, *Accident Analysis and Prevention* 21 (1989) 85–100.
[35] W. McConnell, R. Howard, H. Guzman, J. Bomar, J. Raddin, J. Benedict, H. Smith, C. Hastell, Analysis of human test subject kinematic responses to low velocity rear end impact, presented at *37th Stapp Car Crash Conference*, 1993.
[36] M.W. Scott, W.E. McConnell, H.M. Guzman, R.P. Howard, J.B. Bomar, H.L. Smith, J.M. Benedict, J.H. Raddin, C.P. Hatsell, Comparison of human and ATD head kinematics during low-speed rearend iImpacts, presented at *37th Stapp Car Crash Conference*, 1993.
[37] M. Svensson, P. Lövsund, A dummy for rear-end collisions—development and validation of a new dummy-neck, presented at *IRCOBI Conference*, Verona, Italy, 1992.

[38] J. Thunnissen, M. van Ratingen, M. Beusenberg, E. Janssen, A dummy neck for low severity rear impacts, presented at *15th ESV Conference*, Melbourne, Australia, 1996.
[39] N. Yoganandan, F.A. Pintar, A.J. Sances, L. Voo, J.F. Cusick, Inertial flexion-extension loading of the human neck, *Advance Bioengineering* 31 (1995) 45–46.
[40] T. Matsushita, T.B. Sato, K. Hirabayashi, S. Fujimura, T. Asazuma, X-ray study of human neck motion due to head inertia loading, presented at *38th Stapp Car Crash Conference*, 1994.
[41] O. Boström, M. Krafft, B. Aldman, A. Eichberger, R. Fredriksson, Y. Haland, P. Lövsund, H. Steffan, M. Svensson, C. Tingval, Prediction of neck injuries in rear impacts based on accident data and simulation, presented at *IRCOBI Conference*, Hannover, Germany, 1997.
[42] F. Walz, M. Muser, Biomechanical aspects of cervical spine injuries, presented at *39th Stapp Car Crash Conference*, 1995.
[43] R. Nightingale, D. Camacho, A. Armstrong, J. Robinette, S. Myers, Inertial properties and loading rates affect buckling modes and injury mechanisms in the cervical spine, *Journal of Biomechanics* 33 (2000) 191–197.